Particle-vibration coupling in a basis with resonant states

O. Civitarese and A. G. Dumrauf
Department of Physics, University of La Plata, 1900 La Plata, Argentina

R. J. Liotta
Manne Siegbahn Institute, S-10405, Stockholm, Sweden
(Received 30 March 1992)

Neutron and proton bound states and Gamow resonances (Berggren representation) are used as single-particle states to calculate random-phase approximation (RPA) particle-hole multipole excitations in ^{208}Pb and vertex functions for the coupling between particles and multipole vibrations. Escape widths, corresponding to low-lying one-proton states in the neighborhood of the $Z=82$ shell, are calculated in the framework of the standard particle-vibration coupling model. It is shown that the inclusion of Gamow resonances in the single-particle basis and in the RPA wave functions does not affect the dominant one-particle character of low-lying states of the renormalized spectrum corresponding to the odd-even system, as predicted by the particle-vibration coupling model. This result shows that the Berggren representation is suitable to deal with the particle-vibration coupling mechanism and that it can be applied to the study of high-lying single-particle states as well.

PACS number(s): 21.60.Jz, 27.80.+w

I. INTRODUCTION

The study of formal properties of resonant states and its use in eigenfunction expansions of scattering and reaction amplitudes, started by Berggren years ago [1], has been continued in a series of works by other authors [2–7] and is still a matter of interest in the literature [8–12].

One issue of these studies has been the introduction of Gamow states (GS's), i.e., the solutions of the time independent Schrödinger equation with purely outgoing waves at large distances, as basis elements in the expansion of Green functions. This made it possible to apply Gamow resonances in the study of the continuum in nuclear structure calculations [2–12].

Since Gamow resonances diverge at infinity one has to use a special definition of internal product to deal with these resonances. In this paper, we will not go into the mathematical details of this and similar features related to Gamow resonances. For this, the reader is referred to the references mentioned above. Instead, we will concentrate on the use of GS's as basis elements to describe excitations taking place in the continuum part of nuclear spectra within the framework of the particle-vibration coupling model [13].

The pole expansion of single-particle Green functions in terms of GS's and bound states approximates rather well the corresponding exact Green function if enough resonances are included in the expansion [8,9]. This feature may allow one to use the set of GS's and bound states as a representation, which we call the Berggren representation, to describe nuclear processes [9]. Even the Mittag-Leffler pole expansion of the Green function is adequate, but within this expansion one cannot define random-phase approximation (RPA) wave functions [9]. Moreover, the appearance of antibound states and capturing resonances in the Mittag-Leffler expansion is alien to the ideas that one usually attaches to a basis set of states. This is not the case with the Berggren expansion, where the bound single-particle states in the basis are the same as in the shell model, while the unbound states are outgoing resonances, which is a natural extension of the shell model.

The use of the Berggren representation to describe particle-hole excitations results in a set of equations very similar to the standard RPA equations. This method was thus called [8,10] resonant RPA (RRPA). The quantities calculated within the RRPA agree well with both the corresponding experimental data and with exact calculations [8,9]. It was also found [10] that giant resonances are mainly built upon single-particle states that are bound or quasibound. This explains why bound (harmonic oscillator) representations also reproduce well the position and electromagnetic transitions of the giant resonances. These quantities are determined by the main (bound) components. The limitations of bound representations become apparent when quantities directly related to the continuum (as partial decay widths) are analyzed. In these cases one has to include the continuum explicitly, and the corresponding calculations become difficult and cumbersome [11,14]. However, some of the formal difficulties concerning the treatment of the continuum have been solved recently [20]. A new method is available [20] that allows for the calculation of nonstatistical decay channels. The method of Ref. [20] is based on the coupling between discrete and doorway configurations belonging to the continuum.

The present formalism is based on similar ideas. In our approach we have started from the RRPA and Berggren representations as an alternative way to a complete diagonalization. We have adopted this representation since within the RRPA the calculation of partial decay widths can be conveniently performed [12]. In view of these re-

sults it seems natural to extend the use of Berggren expansions to more complicated excitations. The simplest case beyond particle-hole excitations is two-particle one-hole excitations. These excitations have been thoroughly studied in the past in relation to bound states. In particular, nuclear field theory was shown to be well suited to study these kinds of excitations [13]. We will extend this method to study decay widths of single-particle proton resonances in the lead region.

The formalism is presented in Sec. II, applications are in Sec. III, and the conclusions are in Sec. IV.

II. FORMALISM

In this section, we will present the extension of the nuclear field theory formalism to include excitations lying in the continuum part of nuclear spectra. Since nuclear field theory [13] is based on Green function expansions, the inclusion of the Berggren representation in the formalism is rather straightforward. The set of single-particle states are obtained by solving the Schrödinger equation with the boundary condition of outgoing waves at infinity. For details about normalization and the internal product of Gamow states, see Ref. [10]. Using a separable multipole-multipole interaction of the form

$$V_\lambda(r_1,r_2)=-\kappa_\lambda Q_\lambda(\mathbf{r}_1)\cdot Q_\lambda(\mathbf{r}_2)\ , \tag{1}$$

where

$$Q_{\lambda\mu}(\mathbf{r})=f_\lambda(r)Y_{\lambda\mu}(\hat{\mathbf{r}})\ , \tag{2}$$

the RRPA response function can be written as [9,14]

$$R(E)=\frac{R^0(E)}{1+\kappa_\lambda R^0(E)}\ , \tag{3}$$

where $R^0(E)$ is the uncorrelated particle-hole response function and the strength κ_λ is determined by fitting the energy of a given state, as usual. The uncorrelated response function R^0 is given by [9]

$$R^0(\lambda,E)=\sum_{p,h}|M(\mathrm{ph},\lambda)|^2\int dr\,dr'\,\phi_h(r)f^*_\lambda(r)[g_p(r,r',E+\epsilon_h)+g_p(r,r',-E+\epsilon_h)]\phi_h(r')f_\lambda(r')\ , \tag{4}$$

where p and h label particle and hole states, $g_p(r,r')$ is the single-particle Green function, and the quantity $M(\mathrm{ph},\lambda)$ is the geometrical part of the reduced matrix element of the Q_λ operator.

The energies ω solutions of the RRPA equations are obtained by calculating the poles of the response function $R(E)$, i.e.,

$$R^0(\omega_\lambda)=-1/\kappa_\lambda\ . \tag{5}$$

With the corresponding residues, one then computes the RRPA vertex functions. The widths of the single-particle states proceeds through the coupling with the particle-hole giant resonances. We calculate this coupling as in Ref. [13]. The correction $\delta E(k_1)$ to the energy of the single-particle state k_1 due to coupling to intermediate particle-phonon configurations can be written as

$$\delta E(k_1)=\sum_{k_2,\lambda}\langle k_1|V|(k_2\lambda)k_1\rangle\langle(k_2\lambda)k_1|V|k_1\rangle \times\frac{1}{(\epsilon_{k_1}-\epsilon_{k_2}-\Omega_\lambda)}\ , \tag{6}$$

where k_2 labels the intermediate single-particle states and λ labels the corresponding phonons with energy Ω_λ.

In terms of the RRPA vertex functions $\Lambda_s(k_1,k_2,\lambda)$, one obtains

$$\delta E(k_1)=\sum_{k_2,\lambda}\frac{2\lambda+1}{2k_1+1}\frac{\Lambda_s(k_1,k_2,\lambda)^2}{\epsilon_{k_1}-\epsilon_{k_2}-\Omega_\lambda}\ , \tag{7}$$

where

$$\Lambda_s(k_1,k_2,\lambda)=\sum_{J,p,h}(2J+1)X(\mathrm{ph},\lambda) \times\langle(k_1,h)J|V|(p,k_2)J\rangle\begin{Bmatrix}k_1 & k_2 & \lambda\\ p & h & J\end{Bmatrix} \tag{8}$$

and $X(\mathrm{ph},\lambda)$ are the forward-going amplitudes of the RRPA. In addition to the correction $\delta E(k_1)$, we have to compute the contribution due to exchange. This has to be subtracted [13] from δE because exchange terms have been included in the definition of the two-body matrix elements appearing in the RRPA response function. The contribution due to exchange is

$$\delta E_{\mathrm{exch}}(k_1)=\sum_{k,k',h}\frac{2\lambda+1}{2k_1+1}\frac{\langle(hk_1)\lambda|V|(kk')\lambda\rangle^2}{\epsilon_{k_1}-\epsilon_k-\epsilon_{k'}-\epsilon_h}\ . \tag{9}$$

In the present work we have neglected couplings with holes and pair-addition phonons since, for protons above $Z=82$, such mixings would be possible only with states that belong to orbits that are two shells below the core and that therefore have very large energy denominators.

It is worth stressing that all quantities related to the RRPA solutions are complex. Therefore, the correction $\delta E(k_1)$ to a given external single-particle line will in general be complex even if the external single-particle line would correspond to a bound state. That a bound state can acquire a width can be explained by the fact that the continuum Green function has been replaced, in the present formalism, by the corresponding Berggren pole expansion. Then, the coupling of the bound particle with the phonons will play the role of a doorway to the continuum via the phonon widths. This may be the mechanism that induces the width of deep-lying single-particle states.

III. RESULTS AND DISCUSSION

In this section we present applications of the formalism developed above to study single-particle resonances in the lead region. The single-particle states, which are shown in Table I, have been obtained by using the computer code GAMOW [3]. The parameters of the central Woods-Saxon potential that we have adopted for protons (neutrons) are $a=0.75$ (0.70) fm, $r_0=1.19$ (1.27) fm, and $V_0=66.0$ (44.4) MeV. The bound states in Table I are approximately the same as in other calculations [15] but the states lying in the continuum show the typical behavior expected for resonances. That is, the imaginary part of the energies are negative as they correspond to the widths of the resonances (Gamow states). The widths of proton Gamow states are generally smaller than those corresponding to neutrons, just reflecting the influence of the Coulomb barrier. In the same manner, states with high angular momenta are narrow due to the trapping of the particle by the centrifugal barrier. For even orbital angular momenta the states lie higher as the angular momenta increase. At the same time the widths also increase, as can be seen from the values listed in Table I.

The single-particle states shown in Table I can be considered as a representation to treat processes occurring in the continuum part of nuclear spectra (Berggren representation [8,9]). One can see from Table I that the Berggren representation is a natural extension of the shell-model basis. This can be contrasted with other expansions of the continuum, such as the Mittag-Leffler expansion [9], where bizarre states may appear (e.g., antibound states).

Within the Berggren basis of Table I, we have calculated RRPA response functions corresponding to multipole excitations with $\lambda^{\pi}=2^{+}$, 3^{-}, and 4^{+} in ^{208}Pb. The coupling constants κ_{λ} of the separable multipole-multipole residual interaction, described in the preceding section, have been adjusted to reproduce the observed excitation energies of the first excited states for each of the multipolarities included in the calculation. The experimental values of these energies in ^{208}Pb have been taken from Ref. [16]. In computing the matrix elements of the RRPA response function, we have followed the method of Refs. [8], [10], and [17] to deal with the divergent character of some of the GS's included in the single-particle basis. For the radial dependence of the operator (2), we have adopted the parametrization given in Refs. [8], [10], and [17], with constant values for $f_{\lambda}(r)$, for $6\leq r\leq 8$ fm.

The imaginary part of the RRPA energies are half the widths of narrow particle-hole resonances [12]. In partic-

TABLE I. Set of single-particle states used in the calculations. Bound states and GS's are included in the basis, both for protons and neutrons. The parameters of the Woods-Saxon potential that we used are given in the text.

N	State	ϵ_p (MeV)	ϵ_n (MeV)	N	State	ϵ_p (MeV)	ϵ_n (MeV)
0	$0s_{1/2}$	-37.656	-40.231	7	$2f_{7/2}$	$12.748-i0.652$	$2.078-i0.875$
1	$0p_{3/2}$	-33.547	-36.328	7	$3p_{1/2}$	$13.220-i2.502$	
1	$0p_{1/2}$	-32.926	-35.928	8	$0k_{17/2}$	$14.066-i0.001$	$5.029-i0.001$
2	$0d_{5/2}$	-28.485	-31.749	7	$2f_{5/2}$	$14.650-i1.566$	$2.698-i2.322$
2	$0d_{3/2}$	-27.075	-30.769	7	$0j_{13/2}$	$15.086-i0.005$	$5.411-i0.009$
2	$1s_{1/2}$	-25.296	-29.622	7	$1h_{9/2}$	$15.964-i0.393$	$5.403-i0.726$
3	$0f_{7/2}$	-22.671	-26.609	8	$3d_{5/2}$	$16.615-i8.467$	$7.392-i13.206$
3	$0f_{5/2}$	-20.172	-24.782	8	$4s_{1/2}$	$16.871-i11.907$	$7.206-i15.710$
3	$1p_{3/2}$	-18.320	-23.471	8	$2g_{9/2}$	$17.844-i3.547$	$5.540-i6.376$
3	$1p_{1/2}$	-17.329	-22.695	8	$3d_{3/2}$	$17.848-i10.932$	
4	$0g_{9/2}$	-16.232	-20.991	8	$1i_{13/2}$	$18.143-i0.575$	$7.662-i1.038$
4	$0g_{7/2}$	-12.365	-18.058	8	$2g_{7/2}$	$20.068-i6.638$	$8.343-i11.536$
4	$1d_{5/2}$	-11.038	-17.055	9	$3f_{5/2}$	$20.509-i17.795$	$9.837-i19.000$
5	$0h_{11/2}$	-9.265	-14.960	9	$3f_{7/2}$	$20.845-i16.660$	
4	$1d_{3/2}$	-9.098	-15.513	9	$0l_{19/2}$	$22.343-i0.043$	$12.021-i0.093$
4	$2s_{1/2}$	-8.712	-15.299	8	$1i_{11/2}$	$23.243-i2.520$	$11.330-i3.745$
5	$0h_{9/2}$	-3.784	-10.691	9	$2h_{11/2}$	$23.403-i9.227$	
5	$1f_{7/2}$	-2.584	-10.487	9	$1j_{15/2}$	$24.683-i2.309$	$13.224-i3.518$
6	$0i_{13/2}$	-1.684	-8.572	8	$0k_{15/2}$	$24.819-i0.222$	$13.598-i0.424$
5	$2p_{3/2}$	-0.690	-8.355	8	$3d_{3/2}$		$14.131-i18.919$
5	$1f_{5/2}$	-0.518	-8.078	10	$0m_{21/2}$	$30.697-i0.314$	$19.116-i0.518$
5	$2p_{1/2}$	0.491	-7.413	9	$1j_{13/2}$	$30.849-i6.870$	$18.467-i9.957$
6	$1g_{9/2}$	4.028	-3.926	10	$1k_{17/2}$	$31.493-i5.298$	$19.463-i7.334$
6	$0i_{11/2}$	5.434	-2.797	9	$3f_{7/2}$		$20.605-i20.005$
7	$0j_{15/2}$	5.960	-1.883	9	$0l_{17/2}$		$22.138-i1.723$
6	$2d_{5/2}$	$6.748-i0.002$	-2.072	10	$2i_{13/2}$	$32.485-i18.098$	$25.079-i20.060$
6	$3s_{1/2}$	$7.843-i0.037$	-1.438	9	$0l_{17/2}$	$36.644-i1.229$	
6	$1g_{7/2}$	$8.087-i0.001$	-0.768	10	$3g_{9/2}$	$35.886-i22.146$	$27.582-i23.760$
6	$2d_{3/2}$	$8.530-i0.028$	-0.781	10	$2i_{11/2}$	$37.872-i21.765$	$28.334-i24.554$
7	$1h_{11/2}$	$11.390-i0.022$	$2.251-i0.026$	11	$1l_{19/2}$	$38.960-i9.475$	$26.754-i12.176$
7	$3p_{3/2}$	$12.647-i1.888$		11	$0n_{23/2}$	$39.229-i1.007$	$26.492-i1.360$

ular, this is the case for the giant resonances. This is a remarkable property of the RRPA since the residual interaction induces the mixing of many single-particle configurations in the collective states, and each of these configurations contributes with its own width. In Fig. 1 we present the distribution of the widths as a function of the position of the RRPA states for quadrupole, octupole, and hexadecapole excitations. The large widths seen in this figure have to be interpreted as the continuum background contribution to the particle-hole resonances. This background is actually due to the unperturbed single-particle widths of Table I.

Some of the states shown in Fig. 1 display a large width. They are mostly dominated by a single-particle–hole configuration. Only the states with a narrow width are really collective, in the sense of the percentage of the isoscalar energy weighted sum rule that they have. These are the states that contribute to the energy shift of one-particle states. The percentages of the energy weighted sum rule of each multipole field, for dominant RRPA eigenvalues, are shown in Table II. In general, narrow states between 10 and 15 MeV exhaust most of the energy weighted sum rule [8,10].

We have computed the corrections to the energy of the active states above the shell closure for protons by using Eqs. (6) and (9). We included as intermediate states all single-particle states of Table I and all phonons of Fig. 1 with imaginary parts of the energy (in absolute value) up to 15 MeV. Wider phonon resonances would be part of the proper continuum, and its contribution to the energy shift should be negligible. We have checked this by including states up to 40 MeV wide in the calculation and found that the results that we discuss below are not significantly affected by the wider states.

First, we computed the energy shift corresponding to bound states, which should be real quantities. Yet, one may expect that the renormalization of a bound unperturbed state by the coupling to a particle-hole excitation can result in a large value of the imaginary part of the renormalized energy. This can be produced by either intermediate Gamow resonances or by phonons lying in the continuum (like the giant resonances). However, a calculation performed within a bound representation gives results that agree well with experiment [13,18]. In order to understand in detail the effect of the Gamow resonances in this case we have also used a bound representation. The results obtained with both the Berggren and the bound representation are presented in Table III. As can be seen in this table, our calculation predicts an energy shift similar to that obtained within the bound representation. All multipole fields contribute coherently to the shift, reflecting the isoscalar character of low-lying vibrational states. The corresponding contributions to the width are of the order of tenths of keV, and for some of the states there is a cancellation i.e., for $h_{9/2}$ and $f_{5/2}$.

The values of the corresponding real parts are all negative, showing that the spectrum of bound states is compressed by the particle-vibration coupling, as expected [18].

We have also calculated the energy shift of states lying in the continuum part of the spectrum. In this case, the

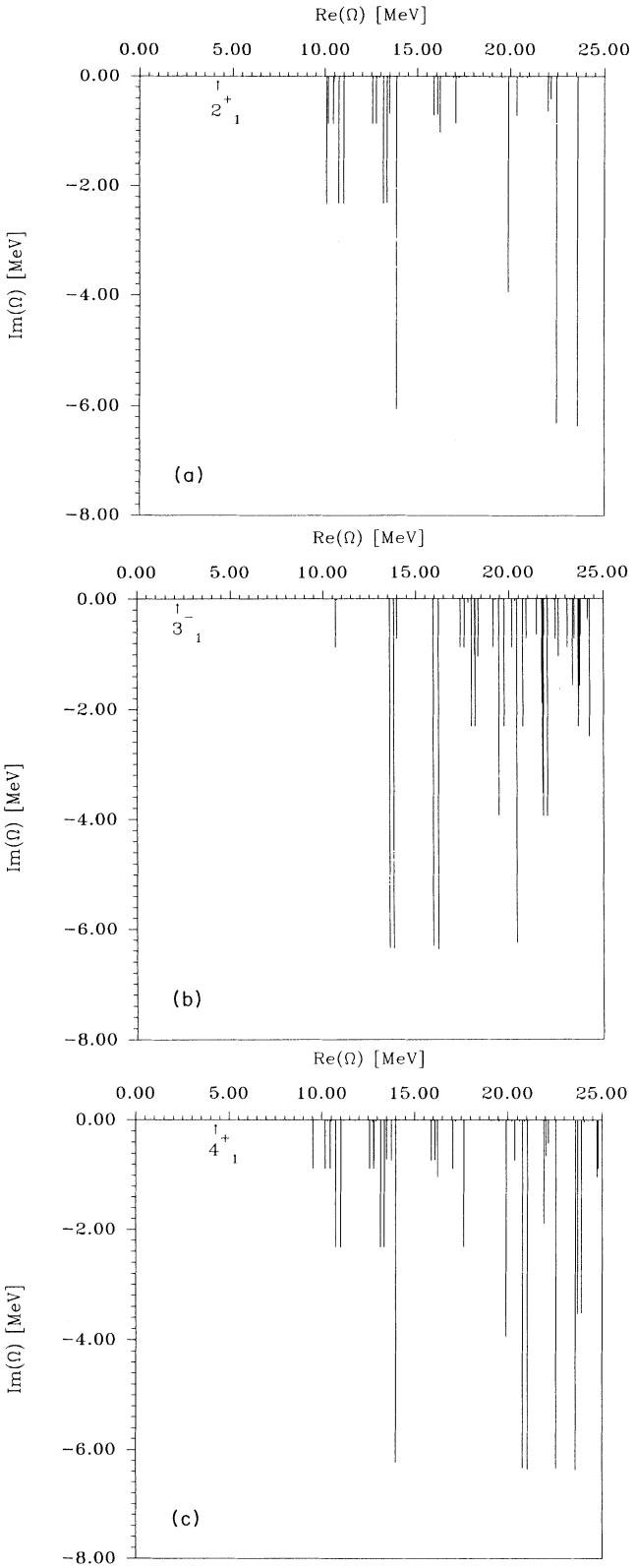

FIG. 1. (a) Real and imaginary parts of the RRPA one-phonon spectrum, for $\lambda^{\pi}=2^{+}$ states, in ^{208}Pb. (b) Real and imaginary parts of the RRPA one-phonon spectrum, for $\lambda^{\pi}=3^{-}$ states, in ^{208}Pb. (c) Real and imaginary parts of the RRPA one-phonon spectrum, for $\lambda^{\pi}=4^{+}$ states, in ^{208}Pb.

imaginary parts give the corrections to the widths of the states. In Table IV we present the results of our calculation for the rather wide states $3p_{3/2}$, $2f_{7/2}$, and $2f_{5/2}$. In these cases one should not expect the bound representation to provide a good description. The cases of Table IV are examples of nuclear processes where the continuum must be included explicitly. This explains the difference between the calculated values performed within the Berggren and the bound representations seen in Table IV. Note that, while in the Berggren representation the intermediate states contribute almost coherently to the energy shift (exactly as in the cases of Table III), the bound representation gives results that differ very much from what it gave in the previous case. The correction to the single-particle widths shown in Table IV are in all cases positive. That is, the particle-vibration coupling tends to narrow the single-particle resonances. Although the present results are qualitatively correct, they are dependent on the approximations that we have used to calculate vertex functions for the particle-vibration coupling (separable multipole-multipole interactions) and they are certainly dependent on the use of Berggren's representation for the treatment of the continuum. In order to gain some quantitative information on the approach, we have computed spectroscopic factors for the low-lying proton states considered in the calculations. The results are shown in Table V. The spectroscopic factors corresponding to calculations using only bound states do not differ much from those obtained with the present representation. This is true for low-lying proton states, since they have small widths, as we have shown before. For states with larger widths the present method leads to very small

TABLE II. Dominant unperturbed particle-hole configurations, phonon excitation energies, and percentages of the isoscalar energy weighted sum rules (EWSR's), for the multipole fields included in the calculations. Neutron (proton) particle-hole configurations have been denoted n (p); unperturbed ($E_{\rm ph}$) and RRPA energies (Ω_n) are given in units of MeV.

$\lambda^\pi=0^+$	$E_{\rm ph}$	Ω_n	% EWSR
$n(2f_{5/2}1f_{5/2})$	$10.758-i2.322$	$10.705-i2.348$	1.51
$n(3s_{1/2}2s_{1/2})$	13.861	12.900	54.70
$n(2d_{3/2}1d_{3/2})$	14.732	13.905	1.86
$n(2d_{5/2}1d_{5/2})$	14.983	$14.798-i0.001$	1.00
$n(1h_{9/2}0h_{9/2})$	$16.094-i0.726$	$15.167-i0.012$	3.65
$\lambda^\pi=2^+$	$E_{\rm ph}$	Ω_n	% EWSR
$n(1g_{9/2}0i_{13/2})$	4.646	4.085	7.23
$p(1f_{7/2}0h_{11/2})$	6.681	$6.365-i0.003$	4.50
$n(2f_{5/2}1f_{5/2})$	$10.760-i2.320$	$10.500-i0.100$	48.80
$\lambda^\pi=4^+$	$E_{\rm ph}$	Ω_n	% EWSR
$n(1g_{9/2}0i_{13/2})$	4.646	4.320	4.15
$n(0i_{11/2}0i_{13/2})$	5.770	5.690	1.20
$n(2d_{5/2}0i_{13/2})$	6.500	$6.290-i0.001$	4.12
$n(1g_{7/2}0i_{13/2})$	7.800	$7.600-i0.003$	7.41
$p(2p_{3/2}0h_{11/2})$	8.570	$7.900-i0.001$	2.94
$n(1h_{11/2}2p_{3/2})$	$10.610-i0.026$	$10.511-i0.020$	2.00
$n(1g_{9/2}2s_{1/2})$	11.370	$11.180-i0.011$	5.73
$n(1g_{9/2}1d_{3/2})$	11.590	$11.540-i0.002$	1.31
$n(2f_{7/2}1f_{7/2})$	$12.580-i0.375$	$11.810-i0.016$	8.17
$n(0k_{17/2}0g_{9/2})$	$26.020-0i.001$	$25.770-i0.020$	1.47
$p(2g_{9/2}2s_{1/2})$	$26.556-i3.547$	$26.585-i0.069$	4.96
$n(2f_{5/2}0f_{5/2})$	$27.462-i2.320$	$27.457-i0.390$	2.00
$n(1k_{17/2}0i_{13/2})$	$28.035-i7.334$	$27.954-i7.342$	1.29
$p(0j_{15/2}0f_{7/2})$	$28.631-i0.001$	$28.566-i0.018$	1.00
$\lambda^\pi=3^-$	$E_{\rm ph}$	Ω_n	% EWSR
$n(1g_{9/2}1f_{5/2})$	4.152	2.610	22.16
$n(0i_{11/2}1f_{5/2})$	5.281	4.615	1.46
$n(2f_{5/2}2s_{1/2})$	$17.979-i2.322$	$17.888-i0.075$	27.31

TABLE III. Real and imaginary parts of the energy shift due to the coupling between particle and phonon states. Contributions to the real and imaginary parts of the shift corresponding to the vibrational fields λ^π for the states indicated in the first column are given. Given in the last column are the corresponding contributions without the inclusion of Gamow states in the single-particle basis. These are real quantities. The energy shifts are given in units of MeV.

State	λ^π	$\mathrm{Re}(\delta E-\delta E_{\mathrm{exch}})$	$\mathrm{Im}(\delta E-\delta E_{\mathrm{exch}})$	$\delta E-\delta E_{\mathrm{exch}}$
$1f_{7/2}$	2^+	−0.100	−0.017	−0.118
	3^-	−0.123	−0.009	−0.227
	4^+	−0.278	−0.007	−0.299
	Total	−0.501	−0.033	−0.644
$0h_{9/2}$	2^+	−0.057	−0.001	−0.059
	3^-	−0.023	−0.001	−0.048
	4^+	−0.136	0.002	−0.152
	Total	−0.216	0.000	−0.259
$0i_{13/2}$	2^+	−0.111	−0.012	−0.141
	3^-	−0.110	−0.012	−0.141
	4^+	−0.310	0.007	−0.353
	Total	−0.531	−0.017	−0.635
$1f_{5/2}$	2^+	−0.223	−0.012	−0.231
	3^-	−0.091	0.002	−0.159
	4^+	−0.459	0.012	−0.541
	Total	−0.773	0.002	−0.931
$2p_{3/2}$	2^+	−0.160	−0.013	−0.199
	3^-	−0.067	−0.004	−0.117
	4^+	−0.510	−0.031	−0.604
	Total	−0.737	−0.048	−0.920

spectroscopic factors, as we have seen from our results. This is the case for the states shown in Table IV.

IV. CONCLUSIONS

In this paper, we have presented a formalism to treat bound and resonant states in a particle-vibration coupling scheme. Both the particle and the phonon states can themselves be resonances, i.e., states with complex energies.

We have found that, although the imaginary part of the single-particle and particle-hole phonon energies may be large, the particle-vibration coupling does not yield unrealistic escape widths for low-lying single-particle

TABLE IV. Real and imaginary parts of the energy shift for the high-lying proton states $3p_{3/2}$, $2f_{7/2}$, and $2f_{5/2}$. The results are shown as in Table III.

State	λ^π	$\mathrm{Re}(\delta E-\delta E_{\mathrm{exch}})$	$\mathrm{Im}(\delta E-\delta E_{\mathrm{exch}})$	$\delta E-\delta E_{\mathrm{exch}}$
$3p_{3/2}$	2^+	−0.000	0.017	−0.005
	3^-	0.007	0.005	−0.025
	4^+	0.031	0.040	−0.032
	Total	0.038	0.062	−0.062
$2f_{7/2}$	2^+	−0.014	0.005	−0.571
	3^-	−0.010	0.021	0.065
	4^+	−0.035	0.030	−0.100
	Total	−0.059	0.056	−0.606
$2f_{5/2}$	2^+	−0.016	0.012	0.012
	3^-	0.008	0.044	−0.043
	4^+	−0.005	0.135	−0.062
	Total	−0.013	0.191	−0.093

TABLE V. Spectroscopic factors for proton states. Spectroscopic factors, for low-lying proton states, obtained in the calculations using (a) only bound states [S_j^2(BS)] [21] and (b) the basis with bound and resonant states [S_j^2(GS)].

State	$S_j^2(B)$	S_j^2(GS)
$h_{9/2}$	0.86	0.95
$f_{7/2}$	0.76	0.88
$i_{13/2}$	0.74	0.90
$f_{5/2}$	0.47	0.52
$p_{3/2}$	0.44	0.70

states. We have found that, for the valence protons in the $Z=82$ shell, the calculated widths are of the order of few keV. The results obtained for the $1f_{7/2}$ and $0i_{13/2}$ states, which are of the order of 60 and 30 keV, respectively, are somehow large values since these states are in fact bound states. This can be due to the approximations since we have replaced Green functions in the continuum by the corresponding Berggren representation. Nevertheless, and in view of the relatively large imaginary part of the single-particle and phonon energies that are included in the basis, the calculated escape widths are not too large. This is because there are strong cancellations among the contributions from components of the different multipole fields to the calculated imaginary part of the energy shift. However, the corresponding partial contributions to the real parts of the energy shifts add up coherently. The resulting values are in agreement with the known systematics extracted from the complete perturbative treatment, which also includes pair collective excitations [13,19,20,21]. We think that these results constitute a good starting point concerning calculations of one-particle escape widths in the continuum by using the particle-vibration coupling model. In this respect, the formalism that we reported above can be compared with other treatments, particularly with the one presented in Ref. [20]. Results of these calculations will be reported elsewhere [19].

ACKNOWLEDGMENTS

This work has been supported in part by the Consejo Nacional de Investigaciones Cientificas y Tecnicas (CONICET) of Argentina.

[1] T. Berggren, Nucl. Phys. **A109**, 265 (1968).
[2] W. J. Romo, Nucl. Phys. **A116**, 618 (1968).
[3] T. Vertse, K. F. Pal, and Z. Balogh, Comput. Phys. Commun. **27**, 309 (1982).
[4] B. Gyarmati, A. T. Kruppa, Z. Papp, and G. Wolf, Nucl. Phys. A **417**, 393 (1984).
[5] E. Hernandez and A. Mondragon, Phys. Rev. C **29**, 722 (1984).
[6] B. Gyarmati, A. T. Kruppa, and Z. Papp, Phys. Rev. C **31**, 2317 (1985).
[7] B. Gyarmati and A. T. Kruppa, Phys. Rev. C **34**, 95 (1986).
[8] T. Vertse, P. Curuchet, O. Civitarese, L. S. Ferreira, and R. J. Liotta, Phys. Rev. C **37**, 876 (1988).
[9] T. Vertse, P. Curuchet, and R. J. Liotta, Phys. Rev. C **42**, 2605 (1990).
[10] P. Curuchet, T. Vertse, and R. J. Liotta, Phys. Rev. C **39**, 1020 (1989).
[11] N. Van Giai and Ch. Stoyanov, Phys. Lett. B **252**, 9 (1990), and references therein.
[12] T. Vertse, P. Curuchet, R. J. Liotta, J. Bang, and N. Van Giai, Phys. Lett. B **264**, 1 (1991).
[13] D. R. Bes, G. G. Dussel, R. P. J. Perazzo, and H. M. Sofia, Nucl. Phys. **A293**, 350 (1977).
[14] S. Yoshida and S. Adachi, Z. Phys. A **325**, 441 (1986).
[15] J. Blomqvist and L. Rydstrom, Phys. Scr. A **31**, 31 (1985).
[16] Nucl. Data Sheets **47**, 806 (1986).
[17] B. Gyamarti and T. Vertse, Nucl. Phys. **A160**, 523 (1971).
[18] A. Bohr and B. R. Mottelson, *Nuclear Structure* (Benjamin, Reading, MA 1975), Vol. 2, Chap. 6, pp. 416–420.
[19] O. Civitarese, A. G. Dumrauf, and R. J. Liotta (unpublished).
[20] N. Van Giai and Ch. Stoyanov, Phys. Lett. B **272**, 178 (1991).
[21] S. Reich, H. M. Sofia, and D. R. Bes, Nucl. Phys. **A233**, 105 (1974).